AIMS Mathematics, 11(6): 18614–18642
DOI: 10.3934/math.2026757
Received: 18 February 2026
Revised: 10 April 2026
Accepted: 18 May 2026
Published: 24 June 2026

https://www.aimspress.com/journal/Math

Research article

Exotic radiative breather solitons in DNA-related dynamics

Umar Muhammad Dauda[1,*], **Hanita Daud**[2], **Hadil Alhazmi**[3], **Nazreen Waeleh** [4] **and Sani Saleh Musa** [5]

[1] Department of Mathematics, Faculty of Computing & Mathematical Sciences, Aliko Dangote University of Science & Technology, Kano, Nigeria
[2] Department of Applied Sciences, Universiti Teknologi PETRONAS, 32610 Seri Iskandar, Malaysia
[3] Department of Mathematical Sciences, College of Science, Princess Nourah bint Abdulrahman University, P.O. Box 84428, Riyadh 11671, Saudi Arabia
[4] Faculty of Electronics and Computer Technology and Engineering, Universiti Teknikal Malaysia Melaka (UTeM), 76100 Durian Tunggal, Melaka, Malaysia
[5] Department of Mathematics, Jigawa State College of Education & Legal Studies, Jigawa, Nigeria

* **Correspondence:** Email: umarmd2021@gmail.com.

Abstract: We employ the variational principle of calculus and continuum approximation approach to generate a useful dynamical equations to describe the dynamics of deoxy-ribonucleic acid (DNA). Based on the choice of temperature dependent potential function, we establish a better understanding of the effect of variations in temperature T on the dynamics of the underlying system. The mathematical model yields a wave packet solution whose nonlinear superposition gives a special kind of "radiative breather soliton" possessing the periodic lossless energy transfer property. The findings show the existence of breathers in DNA dynamics and provide clear reaffirmation of solitary waves in the behaviour of DNA.

Keywords: breather solitons; radiative breathers; radiative wave packets; continuum approximation, modified morse potential; symmetric morse potential; dynamics; temperature effect
Mathematics Subject Classification: 35B38, 35C07, 35K57, 35L05, 35L20

1. Introduction

A key constituent known to affect deoxyribonucleic acid (DNA) dynamics, often overlooked in most of the literature in the past few decades, is thermal variation. However, temperature plays significant roles in its behaviour. The study of nonlinear excitations in biological macromolecules, particularly DNA, has attracted considerable attention due to its relevance in understanding

fundamental biological processes such as transcription, replication, and energy transport. DNA exhibits complex dynamical behaviour arising from the interplay between nonlinear interactions and dispersive effects along the molecular chain. It is indicated that according to Wartell and Benight (1985), the structural variation of DNA is caused by the temperature variations [19]. They demonstrated that the instability of denaturation in the double-helix structure is a consequence of higher temperature. Furthermore, the research by Yakushevich (2004–2006, [22, 23]) extended oversimplified DNA models to level that encompasses behaviours due to temperature variations. This contribution gave rise to a new dimension of dynamics that involves non-linearity.

It is a well-known fact that the stability, replication, and repair of DNA are significantly influenced by vibrational dynamics. Lu et al. (1977, [8]) provided a preliminary emphasis on the role that vibrational modes play in DNA stability. The contemporary work on the dynamics of DNA is carried out by Peyrard and Bishop (1989). Their work highlighted the influence of non-linearity in the DNA denaturation process.

In recent years, there has been increasing interest in the study of coherent structures such as solitons and breathers in nonlinear systems. These structures exhibit remarkable stability and energy localization properties, making them particularly relevant in biological contexts. However, despite extensive studies, the influence of temperature-dependent interactions and their role in shaping nonlinear excitations in DNA remain insufficiently explored.

1.1. Biological relevance

Early theoretical models describing DNA dynamics were primarily based on discrete lattice formulations, where base pair displacements are governed by nonlinear potentials such as the Morse interaction. Notably, nonlinear wave equations derived from these models have been shown to support soliton-like excitations, which are believed to play a role in localized energy transport and DNA breathing phenomena. Most existing studies focus either on purely discrete models, which are computationally intensive and analytically challenging, or on oversimplified continuum models that neglect important physical effects. In particular, the emergence of radiative breather-soliton structures and their energy exchange mechanisms have not been adequately addressed in the literature. Several discrete models have been proposed to describe DNA dynamics, including the Peyrard-Bishop model and its extensions, which incorporate nonlinear potentials to capture hydrogen bond interactions. These models have successfully demonstrated the existence of localized excitations and thermally induced strand separation.

1.2. Mathematical derivations

Continuum approximations of discrete DNA models have led to nonlinear partial differential equations, such as the Sine-Gordon and nonlinear Klein-Gordon equations, which admit soliton and breather solutions. These continuum models provide valuable analytical insight into wave propagation and energy localization mechanisms. Recent studies have further explored the role of nonlinear wave interactions in biological systems, highlighting the importance of coherent structures in mediating energy transfer. However, the incorporation of temperature-dependent effects into the interaction potential remains limited.

In this article, we intend to provide the dynamics of DNA that are temperature-induced. We derive

a DNA-related model, and give descriptions of the temperature effects on the dynamics through the derived model. Furthermore, we study the consequence of the linear and nonlinear superposition of the obtained solution of the model. The purpose of this study is to get a better understanding of the effects of temperature fluctuations on DNA dynamics

Suppose we consider N molecules (particles) of a DNA interacting in a nonlinear manner. It had been established that these DNA molecules interact collectively in some coordinated way, typically in terms of vibrational modes [8]. However, the description of such a phenomenon lacks full consideration of some important factors, such as thermal variation in the dynamical formulation. This kind of setting is different from classical heat problems or even the time fractional version of heat problem, e.g., see [4].

Even though, the energies of individual particles on a small scale are negligible, when considered collectively they could lead to different behaviour. The energy function describing the interaction of a pair of particles is given by a quantity called the Hamiltonian:

$$H(u_n, v_n) = K(u_n, v_n) + V(u_n, v_n),$$

where $K(u_n, v_n)$ and $V(u_n, v_n)$ are, respectively, the kinetic and potential energy of an arbitrary pair of particles displaced at u_n and v_n.

It is known that the molecules of DNA are composed of two strands made up of sugar phosphate molecules (nucleotides). These strands are connected by nitrogenous bases. Each base in a strand finds its counterpart base in the other strand to form a pair called the hydrogen bond or base-pair.

In this work, we extend existing models by introducing a temperature-dependent Morse potential within a variational framework. The resulting nonlinear hyperbolic equation captures both dispersive and nonlinear effects, enabling the study of radiative breather-soliton solutions.

The DNA model is discrete and therefore is modelled by lattice to capture the nonlinearity dynamics of the DNA. One of the first few models for DNA dynamics is from Peyrard and Bishop (P-B) in 1989 [13]. It has been described, there, that the particles are displaced from their initial equilibrium position (perpendicularly). In the P-B model, the displacement of each base pair towards the hydrogen bond, from their equilibrium positions are respectively u_n and v_n. The stretching strand along the hydrogen bonds is described by [13]

$$H = \sum_n \frac{1}{2} m(\dot{u}_n^2 + \dot{v}_n^2) + \frac{k_1}{2}\left[(u_n - u_{n-1})^2 + (v_n - v_{n-1})^2\right] + V(u_n - v_n),$$

where $V(u_n - v_n)$ is a potential function, m is the mass of the bases, and k_1 is a coupling constant along each of the two strands. See Aguero et al. [1] (2008), and the reference therein, for an alternate Hamiltonian formulation.

In the case of the work done in [1, 13], the potential is given by the Morse function [12]. See [9, 10] for other potential functions for intermolecular interactions. The Morse potential is an average potential representing the two or three bonds that connect the two bases in a pair, and this can be estimated from the parameters obtained for the individual bonds by the analysis of the vibrational modes of DNA. The Morse potential found in [1, 13] is

$$V(u_n - v_n) = D_e\left[e^{-a(u_n - v_n)} - 1\right]^2 \tag{1.1}$$

where D_e is some sort of dissociation energy and a is the width of the potential well. The Figure 1 on the left shows the original potential used in the P-B model.

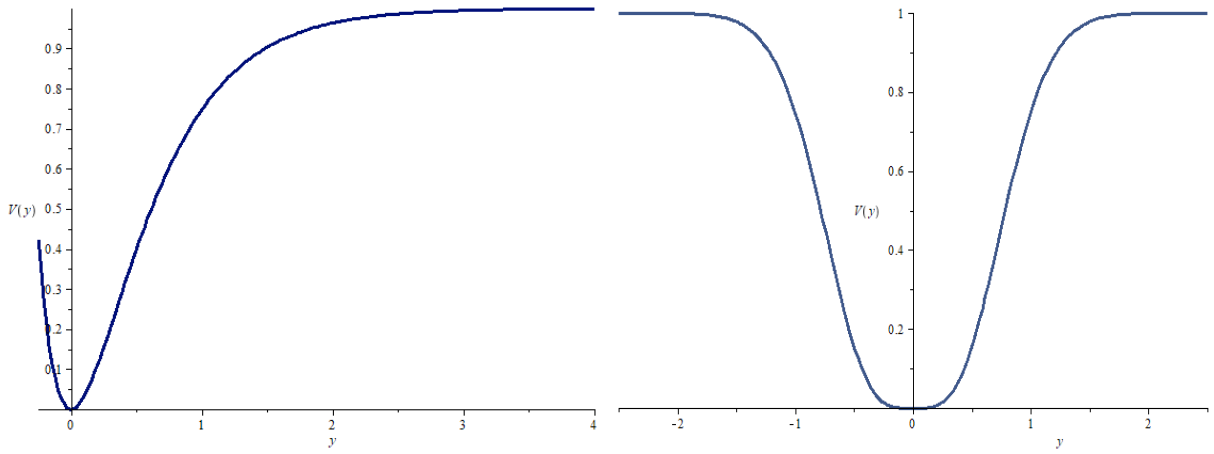

Figure 1. The Morse potentials: (Left) the standard V, (right) symmetric V'.

Solitons, special types of waves that travel through space with their shape and speed retained, are known to exist for the potential dynamic setting; see [2, 13, 20, 21, 24] for more details. In [5], the possibility of existence of soliton excitons in DNA polynucleotides helices has been discovered. Other literature on the presence of solitons and molecular interaction modelling can be found in [2, 6, 7, 14, 16, 18, 25].

Despite significant progress, there remains a lack of comprehensive studies that integrate temperature effects, continuum modelling, and nonlinear coherent structures within a unified framework.

The aim of this study is to develop a continuum dynamical model for DNA that incorporates arbitrary temperature-dependent interactions and investigate the existence and properties of breather-soliton solutions using symmetric and nonsymmetric Morse potential functions. Specifically, we: derive the governing equation using a variational approach, justify the continuum approximation, obtain analytical wave solutions, validate the results numerically, and discuss their physical implications in DNA dynamics.

2. Proposed model

In our case, we assume the potentials whose dissociation energy are temperature dependent $D_e = D_e(T)$ and the potential-width $\alpha = \alpha(T)$ depend on temperature T,

$$V(u_n - v_n) = \frac{D_e(T)}{4}\left[e^{-\alpha(u_n - v_n)} - 1\right]^2, \qquad \alpha = \alpha(T), \tag{2.1}$$

$$V'(u_n - v_n) = \frac{D_e(T)}{4}\left[e^{-\alpha'(u_n - v_n)^2} - 1\right]^2, \qquad \alpha' = \text{const.}, \tag{2.2}$$

where T_0 is the reference temperature and d_{e_0} is the dissociation energy at the reference temperature T_0. The latter form of the Morse potential is symmetric and captures the temperature effect while the

former is the standard Morse potential with the temperature-dependent dissociation energy term. See Figure 1, especially the symmetry potential on the right.

Initially, the Morse potential (1925, [12]) was a model meant to study the vibrational motion of molecules, where D_e is the dissociation energy that represents the depth of the potential well while a controls its steepness. The distance $u_n - v_n$ tells how far apart the two bonding particles are separated from the equilibrium bond length v_n, with an interatomic distance u_n. All together, the Morse potential gives the relationship between two atoms in a diatomic molecule.

Our modified Morse potential plays the role of not only capturing the temperature effect but also the vibrational motion of diatomic molecules and their behaviour in chemical reactions, thereby providing insights into bond strength and molecular dynamics. For instance, the temperature-dependent dissociation term given as

$$D_e = d_e \exp(-T/T_0)$$

indicates that as the temperature T increases, D_e decreases, thereby weakening the bond between the atoms. Likewise, as T decreases, D_e increases thereby strengthening the atomic bond. This temperature dependence reflects the sensitivity of bond strength to thermal fluctuations and provides insights into how temperature affects the stability of the molecules. It is expected that at higher temperatures, the potential well becomes shallower and the molecules are likely to dissociate while at lower temperatures, the potential well becomes deeper, thereby enhancing the stability of the molecule.

The Hamiltonian with respect to the choice of the non-symmetric potential (2.1) now reads as

$$\begin{aligned} H = \sum_n \frac{1}{2}m(\dot{u}_n^2 + \dot{v}_n^2) + \frac{1}{2}k_1[(u_n - u_{n-1})^2 + (v_n - v_{n-1})^2] \\ + \frac{k_2}{4}[(u_n - u_{n-1})^4 + (v_n - v_{n-1})^4] + k_3\frac{D_e}{4}[e^{-\alpha(u_n - v_n)} - 1]^2, \end{aligned} \tag{2.3}$$

for constants k_1, k_2, k_3 related to the coupling (or bonding) and dissociation energy. The positions of the DNA strands are described by the variables

$$x_n = \frac{(u_n + v_n)}{h\sqrt{2}}, \quad y_n = \frac{(u_n - v_n)}{h\sqrt{2}} \quad \text{where} \quad u_n = \frac{h}{\sqrt{2}}(x_n + y_n), \quad v_n = \frac{h}{\sqrt{2}}(x_n - y_n), \tag{2.4}$$

representing, respectively, the in-phase and out-of-phase motions, where y_n is responsible for the stretching of the hydrogen bonds. In these variables, we would have

$$\dot{u}_n = \frac{h}{\sqrt{2}}(\dot{x}_n + \dot{y}_n), \quad \dot{v}_n = \frac{h}{\sqrt{2}}(\dot{x}_n - \dot{y}_n) \implies \frac{1}{2}[\dot{u}_n^2 + \dot{v}_n^2] = h^2(\dot{x}_n^2 + \dot{y}_n^2).$$

Note the canonical forms of H is in terms of the position and momentum of particles variables $p_n = m\dot{x}_n$ and $q_n = m\dot{y}_n$ (not relevant at the moment). The Hamiltonian in the position coordinates x_n and y_n is

$$\begin{aligned} H(x_n, y_n) = \sum_{n=1}^{N} \frac{1}{2}m(\dot{x}_n^2 + \dot{y}_n^2) + \frac{k_1}{2}[(x_n - x_{n-1})^2 + (y_n - y_{n-1})^2] \\ + \frac{k_2}{4}[(x_n - x_{n-1})^4 + (y_n - y_{n-1})^4] + k_3\frac{D_e}{4}[e^{-\alpha(u_n - v_n)} - 1]^2. \end{aligned}$$

The associated Lagrangian in this setting is $\mathcal{L}(y_n, \dot{y}_n) = T - V$ with $T = \sum_n m(\dot{x}_n^2 + \dot{y}_n^2)/2$ given by

$$\mathcal{L}(x_n, y_n) = \sum_{n=1}^{N} \Big[\frac{m}{2}(\dot{x}_n^2 + \dot{y}^2) - \frac{k_1}{2}[(x_n - x_{n-1})^2 + (y_n - y_{n-1})^2] \\ - \frac{k_2}{4}[(x_n - x_{n-1})^4 + (y_n - y_{n-1})^4] - k_3 \frac{D_e}{4}[e^{-\alpha(u_n - v_n)} - 1]^2.$$

When the strand is stretched along the y-coordinate only, the Lagrangian $\mathcal{L}$ and Hamiltonian H are, respectively,

$$\mathcal{L}(y_n, \dot{y}_n) = \sum_{n=1}^{N} \Big[\frac{1}{2} m \dot{y}_n^2 - \frac{k_1}{2} h^2 (y_n - y_{n-1})^2 - \frac{k_2}{4} h^4 (y_n - y_{n-1})^4 - k_3 \frac{D_e}{4} (e^{-2\alpha y_n} - 1)^2 \Big],$$

$$H(y_n, \dot{y}_n) = \sum_{n=1}^{N} \Big[\frac{1}{2} m \dot{y}_n^2 + \frac{1}{2} k_1 h^2 (y_n - y_{n-1})^2 + \frac{1}{4} k_2 [(y_n - y_{n-1})^4] + k_3 \frac{D_e}{4} (e^{-2\alpha y_n} - 1)^2 \Big].$$

We can derive the equation of motion (EOM) via the Hamilton's equations in canonical form:

$$\dot{q}_n = \frac{\partial H}{\partial p_n}, \qquad \dot{p}_n = -\frac{\partial H}{\partial q_n}, \tag{2.5}$$

or by using the Euler -Lagrange (EL) equation with respect to the position coordinates y_n:

$$\frac{d}{dt}\Big[\frac{\partial \mathcal{L}}{\partial \dot{y}_i}\Big] - \frac{\partial \mathcal{L}}{\partial y_i} = 0 \quad \text{for } i = 1, 2, \cdots, N.$$

This amounts to, using the latter,

$$\sum_n \frac{d}{dt}[m\dot{y}_i] - \sum_n \frac{\partial}{\partial y_i}\Big[- \frac{1}{2} k_1 h^2 [(y_n - y_{n-1})^2 - \frac{1}{4} k_2 h^4 [(y_n - y_{n-1})^4] - \frac{D_e}{4}(e^{-2\alpha y_n} - 1)^2 \Big] = 0.$$

The second term, dropping the minus sign, is simplified as follows:

$$\sum_n \frac{\partial}{\partial y_i}\Big[\frac{k_1 h^2}{2}[(y_n - y_{n-1})^2] + \Big[\frac{k_2 h^4}{4}[(y_n - y_{n-1})^4] + D_e(T)(e^{-2\alpha y_n} - 1)^2\Big] \\ = \frac{k_1 h^2}{2} \sum_n [2(y_n - y_{n-1}) \cdot (\delta_{i,n} - \delta_{i,n-1})] + \frac{k_2 h^4}{4} \sum_n [4(y_n - y_{n-1})^3 \cdot (\delta_{i,n} - \delta_{i,n-1})] \\ + \sum_n \Big[\frac{D_e}{4} \cdot 2(e^{-2\alpha y_n} - 1)(-2\alpha e^{-2\alpha y_n} \delta_{i,n})\Big] = 0.$$

Simplifying further, we get

$$k_1 h^2 \sum_n [(y_n - y_{n-1})\delta_{i,n} - (y_n - y_{n-1})\delta_{i,n-1}] + k_2 h^4 \sum_n [(y_n - y_{n-1})^3 \delta_{i,n} - (y_n - y_{n-1})\delta_{i,n-1}] \\ - \sum_n \Big[D_e \alpha e^{-2\alpha y_n}(e^{-2\alpha y_n} - 1)\delta_{i,n}\Big] \\ = k_1 h^2 [(y_i - y_{i+1}) - (y_{i-1} - y_i)] + k_2 h^4 [(y_i - y_{i+1})^3 - (y_{i-1} - y_i)^3] \\ - D_e \alpha e^{-2\alpha y_i^2}(e^{-2\alpha y_i^2} - 1) \\ = -k_1 h^2 (y_{i+1} + y_{i-1} - 2y_i) + k_2 h^4 [(y_i - y_{i+1})^3 - (y_{i-1} - y_i)^3] \\ - D_e \alpha e^{-2\alpha y_i}(e^{-2\alpha y_i} - 1).$$

Combining these results, we get

$$m\frac{\partial^2 y_i}{\partial t^2} - k_1h^2(y_{i+1} + y_{i-1} - 2y_i) + k_2h^4[(y_i - y_{i+1})^3 - (y_{i-1} - y_i)^3] \\ - D_e\alpha e^{-2\alpha y_i}(e^{-2\alpha y_i} - 1) = 0,$$

or

$$\frac{\partial^2 y_i}{\partial t^2} - \alpha_1(y_{i+1} + y_{i-1} - 2y_i) + \alpha_2[(y_i - y_{i+1})^3 + (y_{i-1} - y_i)^3] \\ - 2\alpha\gamma(T)e^{-2\alpha y_i}(e^{-2\alpha y_i} - 1) = 0, \tag{2.6}$$

where $\alpha_1 = \frac{k_1h^2}{m}$, $\alpha_2 = \frac{k_2h^4}{m}$, and $\gamma(T) = \frac{D_e(T)}{2m}$.

Next, by using the standard continuum approximation, we assume $y_n \to y(t, x)$, and using the scaled variable $z = x/h$, we take the following approximation:

$$y_{n\pm1} \approx y(z,t) \pm \varepsilon\frac{\partial y(t,z)}{\partial z} + \frac{\varepsilon^2}{2}\frac{\partial^2 y(t,z)}{\partial z^2} \pm \frac{\varepsilon^3}{6}\frac{\partial^3 y(t,z)}{\partial z^3} + \cdots,$$

where terms up to $O(\varepsilon^2)$ are retained for some small parameter ε. Then,

$$\begin{aligned} y_{i+1} + y_{i-1} - 2y_i &\approx \left[y + \frac{\partial y}{\partial z} + \frac{1}{2}\frac{\partial^2 y}{\partial z^2}\right] + \left[y - \frac{\partial y}{\partial z} + \frac{1}{2}\frac{\partial^2 y}{\partial z^2}\right] - 2y = \frac{\partial^2 y}{\partial z^2} \\ (y_i - y_{i+1})^3 - (y_{i-1} - y_i)^3 &\approx -3\left(\frac{\partial y}{\partial z}\right)^2\left(\frac{\partial^2 y}{\partial z^2}\right) - \frac{1}{4}\left(\frac{\partial^2 y}{\partial z^2}\right)^3 \approx -3\left(\frac{\partial y}{\partial z}\right)^2\left(\frac{\partial^2 y}{\partial z^2}\right), \end{aligned}$$

where, the third and higher-order terms are neglected.

Thus, the equation of interest becomes

$$\frac{\partial^2 y}{\partial t^2} - \left[\alpha_1 + 3\alpha_2\left(\frac{\partial y}{\partial z}\right)^2\right]\left(\frac{\partial^2 y}{\partial z^2}\right) - 2\alpha\gamma(T)e^{-2\alpha y}(e^{-2\alpha y} - 1) = 0, \tag{2.7}$$

with the temperature T and $\gamma(T) = D_e(T)/m$ being governed by the relation

$$D_e(T) = e_0 + e_1(T - T_0) + e_2(T - T_0)^2 + e_3e^{-\alpha(T-T_0)}.. \tag{2.8}$$

Thus, the first term e_0 represents the depth of the base-potential at reference temperature T_0, while e_1, e_2 and e_3 capture, respectively, the linear, quadratic and exponential dependences with $\alpha > 0$ is the rate of exponential-decay.

These terms, linear, quadratic, and exponential, cause variation in $D_e(T)$ with respect to T; thus, there may be some possible physical interpretations. The linear term $e_0 + e_1(T - T_0)$ captures the small linear variation in $D_e(T)$, convenient for negligible temperature variation. The possible anharmonic effects are captured by the quadratic terms, while the rapid decrease in $D_e(T)$ with an increase in the temperature is responsible by the exponential term. Moreover, the latter is also convenient for capturing the thermal weakening of the interactions that may involve a denaturation transition or melting in the DNA.

2.1. Justification of the continuum approximation

The DNA molecule is fundamentally a discrete system consisting of base pairs arranged along a helical backbone. Accordingly, its dynamics can be described using discrete variables $u_n(t)$ representing the displacement of the n-th base pair from its equilibrium position. However, under certain physically relevant conditions, it is appropriate and advantageous to approximate the discrete system by a continuous field.

From the physical point of view, the continuum approximation is valid when the base-pair spacing $a \ll \lambda$, where λ is the wavelength of the excitations. As a result, the DNA excitations (phonons, solitons) extend over many base pairs. Hence, for longwave excitations, the displacement varies slowly across lattice sites, allowing the discrete variable $u_n(t)$ to be approximated by a continuous field $u(x, t)$.

When the characteristic wavelength λ of excitations propagating along the DNA chain is much larger than the lattice spacing a, i.e.,

$$\lambda \gg a := \varepsilon,$$

the displacement field varies slowly between adjacent lattice sites. In this regime, the discrete variable $u_n(t)$ can be approximated by a continuous function:

$$u_n(t) \approx u(x, t), \quad x = na.$$

Using a Taylor series expansion, we write

$$u_{n\pm1}(t) = u(x, t) \pm au_x + \frac{a^2}{2}u_{xx} + O(a^3).$$

Substituting this expansion into the discrete equations of motion and retaining terms up to $O(a^2)$ yields a nonlinear partial differential equation governing the evolution of $u(x, t)$.

The advantages of our approach are both mathematical and analytical. While discrete models capture microscopic lattice effects, they are often analytically intractable, particularly when investigating nonlinear coherent structures such as solitons and breathers. The continuum approximation enables the use of well-established analytical techniques, including: travelling wave reduction, perturbation methods, and stability and modulation analysis. These tools facilitate the derivation of explicit solutions and provide deeper insight into the qualitative behaviour of the system.

Experimental and theoretical studies indicate that nonlinear excitations in DNA, such as localized openings (DNA breathing), extend over several base pairs. This justifies the continuum approximation as an effective description of mesoscopic dynamics, where collective behaviour dominates over individual lattice effects.

It is important to note that the continuum model neglects strong discreteness effects such as lattice pinning and Peierls barriers. However, for the class of long-wavelength excitations considered in this work, the approximation remains valid and physically meaningful.

The question of whether Eq (2.7) is dispersive depends on the nonlinearity; for more details read about dispersion relation for biharmonic equation [15]. It is indeed a wave equation but can lead to a variety of phenomena such as dispersion, modulation instability, and nonlinear interactions. For weaker nonlinearity, Eq (2.7) is nondispersive, particularly when $\alpha_2 \sim 0$, and the equation resembles the classical wave equation with nonlinearity, which is known to be dispersionless. However, the nonlinearity when strong could introduce dispersive effects depending on how it modifies the mode of propagation of different components of y.

3. Travelling-wave and radiative wave solutions

If we remember that Eq (2.7) admits a travelling wave solution, we use the transformation $\xi = z - ct$, for some constant c, and $y(z,t) \equiv V(\xi)$ yields

$$(c^2 - \alpha_1)\frac{d^2V}{d\xi^2} - 3\alpha_2\left(\frac{dV}{d\xi}\right)^2\left(\frac{d^2V}{d\xi^2}\right) - 2\alpha\gamma e^{-2\alpha V}(e^{-2\alpha V} - 1) = 0.$$

Multiplying by $\frac{dV}{d\xi}$ and integrating both-sides, we get

$$(c^2 - \alpha_1)\int V_{\xi\xi}V_\xi d\xi - 3\alpha_2\int V_\xi^3 V_{\xi\xi}d\xi - 2\alpha\gamma\int e^{-2\alpha V}(e^{-2\alpha V} - 1)V_\xi d\xi = -C_1$$

where C_1 is a constant of integration. This yields

$$\frac{(c^2 - \alpha_1)}{2}V_\xi^2 - \frac{3}{4}\alpha_2 V_\xi^4 + \gamma(T)e^{-2\alpha V}(e^{-2\alpha V} - 2) = -C_1.$$

Note that the term in $T = T(t)$ is treated as independent of ξ as it is a function of t not ξ.

Introducing the variable

$$\varphi := e^{-2\alpha V} \tag{3.1}$$

suggests that

$$V = -\frac{1}{2\alpha}\ln\varphi, \qquad V_\xi^2 = \frac{1}{4\alpha^2}\cdot\frac{\varphi_\xi^2}{\varphi^2} \quad \text{and} \quad V_\xi^4 = \frac{1}{16\alpha^4}\cdot\frac{\varphi_\xi^4}{\varphi^4}.$$

The new transformation leads to a new equation of the form

$$-\frac{3}{48\alpha^4}\frac{\varphi_\xi^4}{\varphi^4} - \frac{(\alpha_1 - c^2)}{8\alpha^2}\frac{\varphi_\xi^2}{\varphi^2} + \gamma(T)\varphi(\varphi - 2) = -C_1.$$

or simply

$$A\varphi_\xi^4 + B\alpha^2\varphi^2\varphi_\xi^2 - \gamma(T)\alpha^4\varphi^5(\varphi - 2) - C_1\alpha^4\varphi^4 = 0.$$

where $A = 3/48$, $B = -(c^2 - \alpha_1)/8$, and $\gamma(T) = D_e(T)/2m$.

To find a solitary wave solution that's temperature dependent, we impose the condition that $\varphi_\xi \to 0$ as $\xi \to \pm\infty$, with $\varphi \to 1$ (since as $\lim_{\xi\to\infty} V(\xi) = 0, \varphi = e^{-2\alpha V} \to 1$). This yields

$$A\varphi_\xi^4 + B\alpha^2\varphi^2\varphi_\xi^2 - \gamma\alpha^4\varphi^4(\varphi - 1)^2 = 0.$$

Let us take $(\varphi - 1)^2 \equiv (1 - \varphi)^2$ for some reason to be discussed later. Solving the quartic equation in φ_ξ we get

$$\varphi_\xi^2 = \frac{-B\alpha^2\varphi^2 \pm \sqrt{B^2\alpha^4\varphi^4 - 4A[-\gamma\alpha^4\varphi^4(\varphi - 1)^2]}}{2A} = \frac{\alpha^2\varphi^2(-B \pm \sqrt{B^2 + 4A\gamma(1 - \varphi)^2})}{2A}. \tag{3.2}$$

Since φ_ξ^4 goes to zero as $\xi \to \pm\infty$ faster than φ_ξ^2, we assume $\varphi_\xi^2 \to \varepsilon$ (negligibly small) so that $\varphi_\xi^4 \to 0$ and $\varphi \to 1$. This condition yields $B = 0$, and the Eq (3.2) reduces to

$$\frac{\varphi_\xi^2}{\varphi^2} = \lambda(T)(1 - \varphi), \qquad \text{where } \lambda_\pm(T) := \pm\alpha^2\sqrt{\frac{\gamma}{A}}. \tag{3.3}$$

This equation is simplified to

$$\frac{1}{\sqrt{\lambda_\pm}}\frac{d\varphi}{\varphi\sqrt{(1-\varphi)}} = d\xi.$$

Upon integrating the equation over $[0, \xi]$ and substituting $\varphi = \tanh^2\Theta(\xi) + 1$, one gets,

$$-\frac{2\tanh^{-1}\left(\sqrt{1-\varphi(\xi)}\right)}{\sqrt{\lambda_\pm}} = \xi \quad \Longrightarrow \quad \varphi(\xi) = 1 - \tanh^2\left(-\frac{\sqrt{\lambda_\pm}}{2}\xi\right).$$

The general solution reads as

$$y_\pm(t,z) = -\frac{1}{2\alpha}\ln\left[1-\tanh^2\left(-\frac{\sqrt{\lambda_\pm}}{2}(z-ct)\right)\right], \quad \alpha = \alpha(T), \quad \lambda_\pm = \lambda_\pm(T), \tag{3.4}$$

where $\lambda_\pm(T)$ is as defined in (3.3).

The other possible solution, especially, when $(\varphi-1)^2$ is used instead of $(1-\varphi)^2$, though they are the same, is

$$\tilde{y}_\pm(t,z) = -\frac{1}{2\alpha}\ln\left[1+\tan^2\left(\frac{\sqrt{\lambda_\pm}}{2}(z-ct)\right)\right]. \tag{3.5}$$

At the fixed temperature $T_0 = 310.15$K and $T = 293.15$K, with the $De(T)$ as defined in Eq (2.8), we explore the temperature effect for various values of e_k, $k = 0, \cdots, 3$ while fixing

$$\alpha(T) = \beta_0 + \frac{\beta_1}{1+e^{-\beta_2 T}}. \tag{3.6}$$

Another representation of $\alpha(T)$ used is

$$\alpha(T) = \beta_0 + \beta_1(T - T_0). \tag{3.7}$$

It appears that the solution y_- shown in Figure 2 is the most relevant one. Thus, the linear superposition of $y_\pm$ will be proportional to y_-. It has, however, shown that the solutions are controlled by the nature of $\alpha(T)$, for instance when Eqs (3.6) and (2.8) are used. The dissociation energy $D_e(T)$ is totally controlled by the quadratic term $e_2(T-T_0)^2$; hence, the temperature variation is relevant for the evolution of $y_-(t,z)$. The wave train is apparently a breather-type soliton similar to that of Sine-Gordon's equation. Such types of solutions are found in recent literature (Cahbchoub et al., [3], 2021) and radiation properties of such a wave were studied in Mohammad et al. 2012 [11].

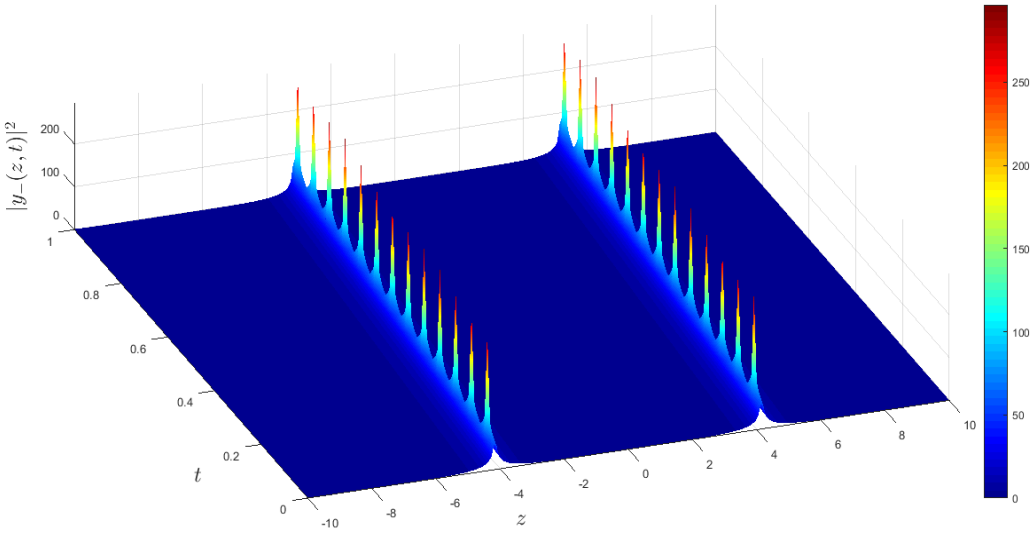

sy

Figure 2. A wave train representation of y_- at $c_1 = 0.75, c_2 = 1$ at the temperature $T_0 = 290.15$ and $T = 300.15$, $h = 0.01$, $e_k = 1$ for $k = 0, \ldots, 3$, where $\alpha(T) = \beta_0 + \beta_1(T - T0)$ with $\beta_0 = -0.06$ and $\beta_1 = -0.05$.

4. Nonlinear superpositions and radiative-waves

Here, we construct nonlinear superpositions $y_\pm$, similarly to [17]. The linear superposition of $y_\pm$ is one we define by

$$y_{\text{sup}} = c_1 y_-(t, z) + c_2 y_+(t, z).$$

The equivalent form of this superposition is

$$y_{\text{sup}} = -\frac{1}{2\alpha}\left\{c_1 \ln\left[1 - \tanh^2\left(-\frac{\sqrt{\lambda_-}}{2}(z - c_- t)\right)\right] + c_2 \ln\left[1 - \tanh^2\left(-\frac{\sqrt{\lambda_+}}{2}(z - c_+ t)\right)\right]\right\}. \tag{4.1}$$

In Figure 2, one sees a moving wave train travelling in a particular direction and nothing much is going on, even for the interaction of the two solitons via the linear superposition. This result is obtained with $k_1 = 0.23$ and $k_2 = 0.0623$ with $m = 230$ and $h = 0.01$.

For the nonlinear superposition, we define

$$y_{\text{pm}} = \frac{1}{1 + c_1 y_-^2(t, z) + c_2 y_+^2(t, z)},$$

for which the result is shown in the Figure 3. y_+ and y_- are the 1-soliton solutions (3.4) of the equation.

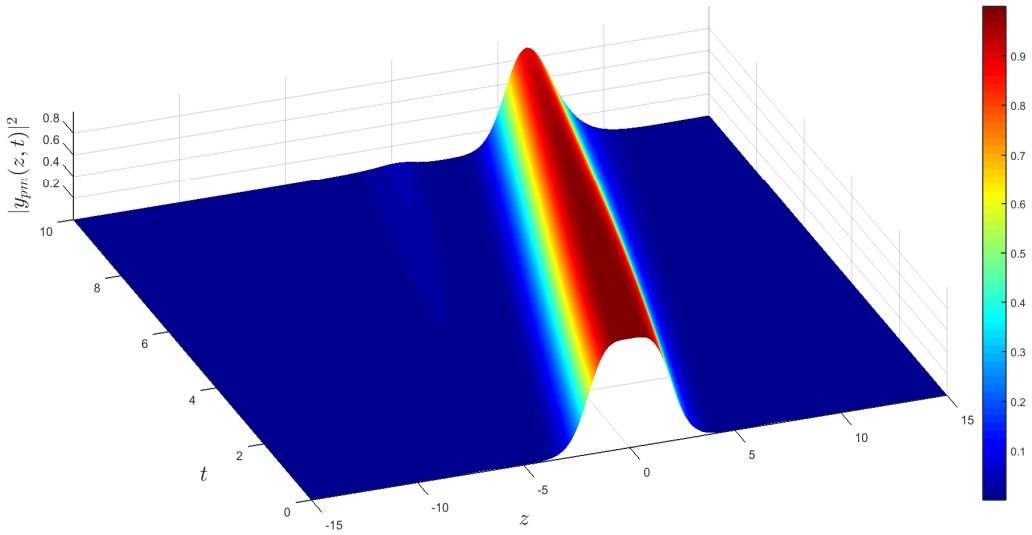

Figure 3. The evolution of y_{pm} at $c_1 = 0.5, c_2 = 0.75$ at the temperature $T_0 = 310.15$ and $T = 293.15$, $h = 0.01$, $e_k = 1$ for $k = 0, \ldots, 3$, where $\alpha(T) = \beta_0 + \beta_1/(1 + \exp(-\beta_2 T))$ with $\beta_0 = \beta_1 = -0.05$ and $\beta_2 = 0.1$.

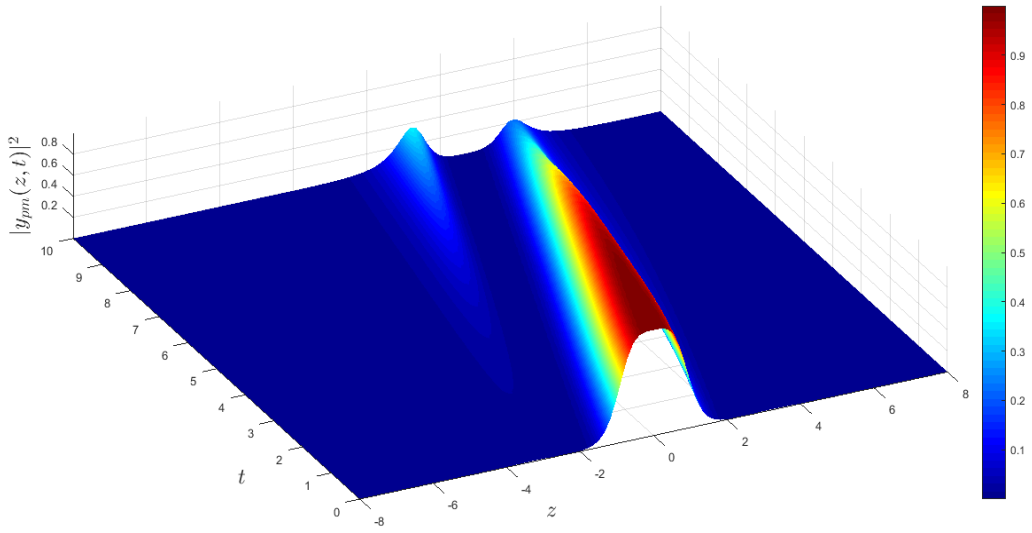

Figure 4. The absolute complex evolution plot of y_{pm} at $c_1 = 0.5, c_2 = 0.75$ at the temperatures $T_0 = 293.15$ and $T = 310.15$, $h = 0.01$, $e_k = 1$ for $k = 0, \ldots, 3$.

The remarkable behaviour of energy exchange and mutual interaction between and among DNA's solitons is also found in the case when $T_0 = 293.15$ and $T = 310.15$. This result is shown in Figure 4. This behaviour is known to be exhibited by breather-type of non-linear waves. It shows that while the travelling wave evolves with great speed, a new travelling wave emerges and causes the initial wave to

lose its energy. As they both evolve, the newly-emerged wave grows to some height while the initial wave begins to lose its energy. They seem to continue propagating in this periodic manner. This result indicates that in the dynamics of DNA, the traveling wave may tend to decompose into two (possibly more) smaller waves, and they keep exchanging the energy among themselves while they evolve.

It is worth noting that this is not surprising for this dynamical equation to admit this kind of periodic solution, also known as breathers. The underlying evolution equation resembles the well-known Sine-Gordon equation except they have a different form of nonlinearities.

Figures 4 and 5 show that the choices of $\alpha(T)$ and that of the reference temperature T_0 have great impact on the behaviour of the dynamics $y(t, z)$. This is evident from the time at which the newly formed travelling wave emerges, particularly when Figure 3 is considered.

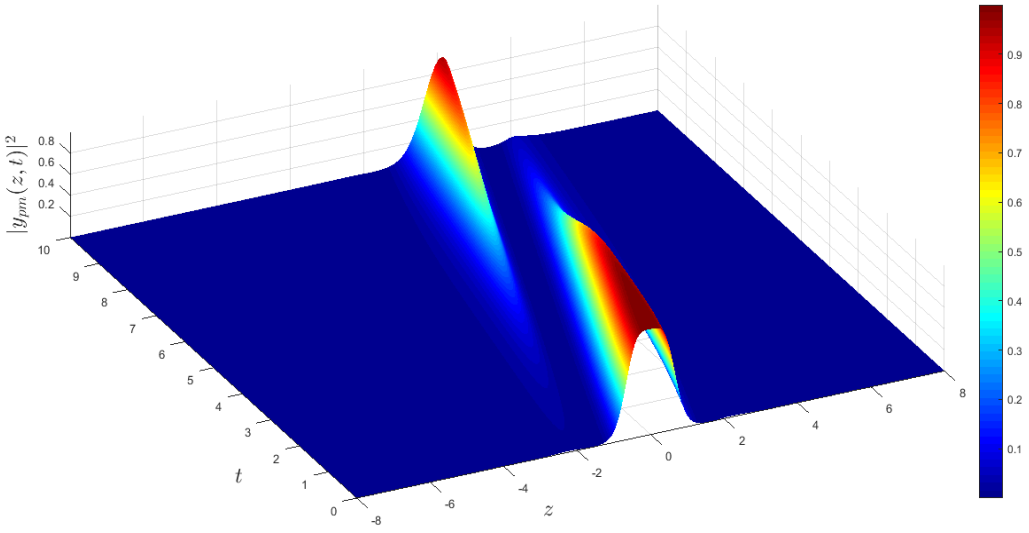

Figure 5. The breather-soliton y_{pm} at $c_1 = 0.5, c_2 = 0.75$ at the temperature $T = 310.15$ and $T_0 = 293.15$, $h = 0.01$, $e_k = 1$ for $k = 0, \ldots, 3$, where $\alpha(T) = \beta_0 + 1/(1 + \beta_1 T)$ with $\beta_0 = \beta_1 = -0.05$.

Figures 6 and 7 represent the time evolution of the radiative breather solitons at different speeds c_- and c_+, and $\alpha(T)$ for temperature T. The results capture a single wave as a simple lump in Figure 6 and the wave train shown in Figure 7 due to superpositioning.

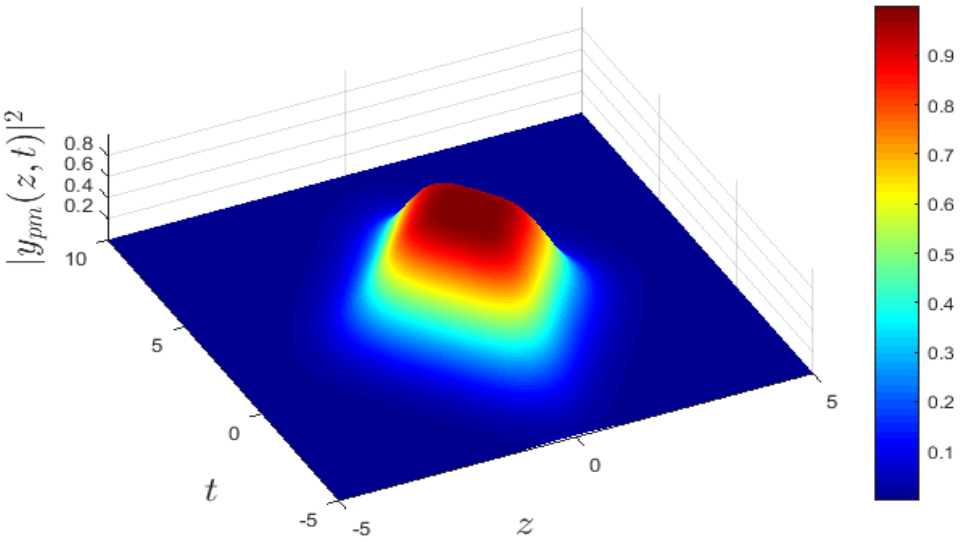

Figure 6. A single breather soliton as *radiative-wave* y_{pm} at speeds $c_- = -0.5$ and $c_+ = 4.5$ with $c_1 = 0.5, c_2 = 0.75$ at the temperatures $T = 310.15$ and $T_0 = 293.15$, $h = 0.01, m = 1$, $e_k = 1$ for $k = 0, \ldots, 3$, where $\alpha(T) = \beta_0 + 1/(1 + \beta_1 T)$ with $\beta_0 = \beta_1 = -0.05$.

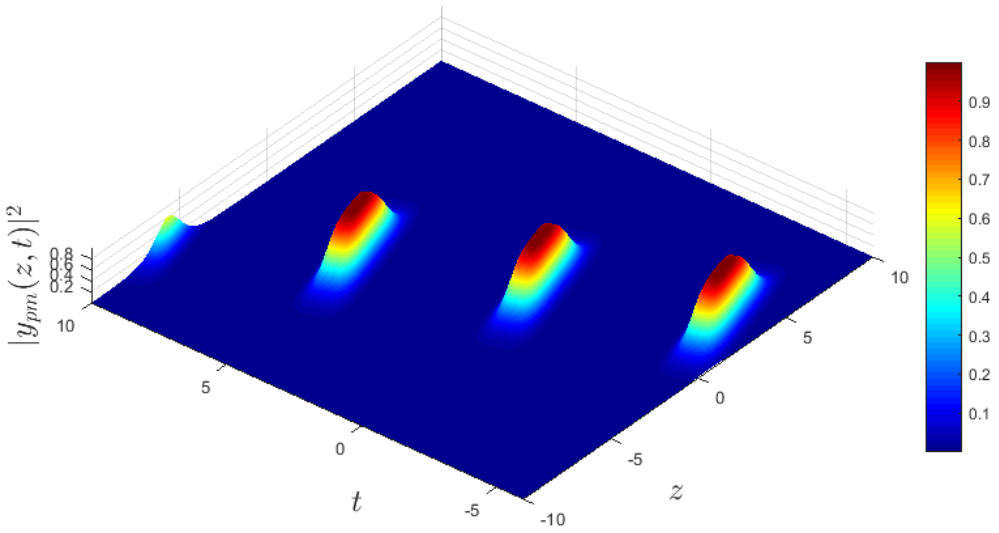

Figure 7. Radiative breather soliton y_{pm} at speeds $c_- = -0.5$, $c_+ = 4.5$ units $c_1 = -0.5, c_2 = 0.5$ at the temperatures $T = 310.15$ and $T_0 = 293.15$, $h = 0.01, m = 1$, $e_k = 1$ for $k = 0, \ldots, 3$, where $\alpha(T) = \beta_0 + 1/(1 + \beta_1 T)$ with $\beta_0 = \beta_1 = -0.05$.

Perhaps, one of the best ways to construct the nonlinear superpositions is via the Bäcklund transformation. There, one uses the existing solution to construct the interacting ones, like

the 2-soliton solutions. It can further be extended to the multi-soliton class of solutions via such a transformation.

The Bäcklund transformation is an essential tool that could somewhat be used to generate a 2-soliton solution, showing the interaction of a 2-soliton characterized by λ_+ and λ_-. This solution would describe their dynamics within the framework of the derived dynamical equation.

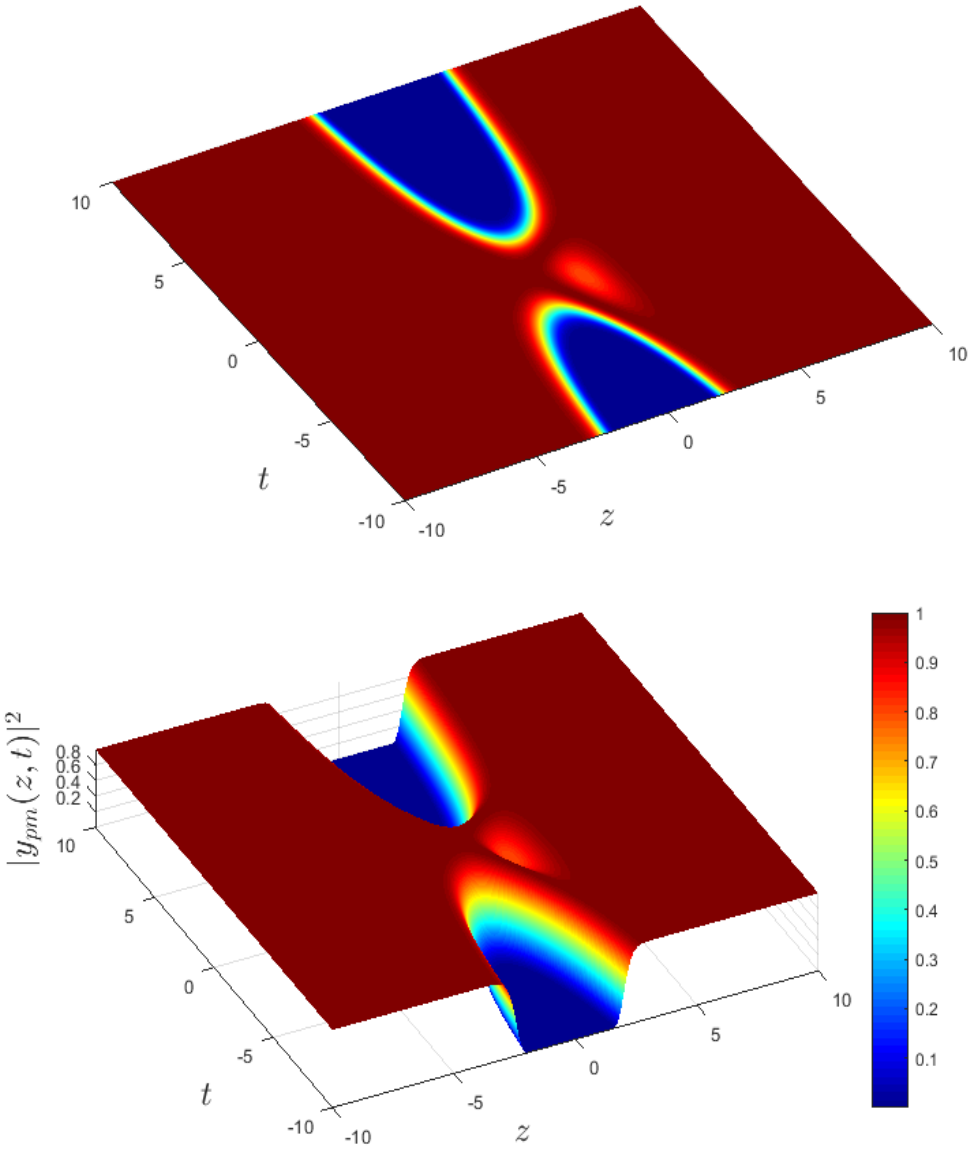

Figure 8. Top view (top) and 3D view (bottom) of a radiative kink soliton y_{pm} at speeds $c_- = 1.5, c_+ = -0.5$ units $c_1 = 1, c_2 = 1$ at the temperature $T = 310.15$ and $T_0 = 293.15$, and $h = 0.01, m = 1, e_k = 1$ for $k = 0, \ldots, 3$, where $\alpha(T) = \beta_0 + 1/(1+\beta_1 T)$ with $\beta_0 = \beta_1 = -0.05$.

The views of the nonlinear superpositioning of the form

$$y_{pm}(t, z) = (c_1 y_+ \cdot c_2 y_-) \cdot \exp(-z^2)$$

with slow radiation tail factor $\exp(-z^2)$ generates a kink-type soliton as shown in the Figure 8.

5. Dynamical equation: Symmetric Morse potential

Here, we consider the symmetric potential (2.2) where the variational approach on the Hamiltonian with the modified symmetric potential (2.2) yields the dynamical equation, $\alpha(T) = a$:

$$\frac{\partial^2 y}{\partial t^2} - \left[\alpha_1 + 3\alpha_2\left(\frac{\partial y}{\partial z}\right)^2\right]\left(\frac{\partial^2 y}{\partial z^2}\right) - 2a\gamma(T)e^{-2ay^2}(e^{-2ay^2} - 1)y = 0, \tag{5.1}$$

with the temperature variable T and $\gamma(T) = D_e(T)/m$ being governed by the relation (2.8).

Let us explore other possible travelling wave solutions. Using the characteristic coordinates $x = z - ct$, the obtained equation becomes

$$\frac{(c^2 - \alpha_1)}{2}V_\xi^2 - \frac{3}{4}\alpha_2 V_\xi^4 + \alpha_3\frac{\gamma(T)}{4a}e^{-2aV^2}(e^{-2aV^2} - 2) = C_1.$$

Introducing the variable

$$\varphi := e^{-2aV^2} \tag{5.2}$$

suggests that

$$V^2 = -\frac{1}{2a}\ln\varphi, \qquad V_\xi^2 = -\frac{1}{8a}\frac{1}{\ln\varphi}\cdot\frac{\varphi_\xi^2}{\varphi^2} \quad \text{and} \quad V_\xi^4 = \frac{1}{64a^2}\frac{1}{(\ln\varphi)^2}\cdot\frac{\varphi_\xi^4}{\varphi^4}.$$

The new transformation leads to a new equation of the form

$$-\frac{3\alpha_2}{256a^2}\frac{1}{(\ln\varphi)^2}\frac{\varphi_\xi^4}{\varphi^4} - \frac{(c^2 - \alpha_1)}{16a}\frac{\varphi_\xi^2}{\varphi^2\ln\varphi} + \alpha_3\frac{\gamma(T)}{4a}\varphi(\varphi - 2) = C_1,$$

or

$$A\varphi_\xi^4 + B\varphi^2\ln(\varphi)\varphi_\xi^2 - [C\gamma(T)\varphi(\varphi - 2) - C_1]\varphi^4\ln(\varphi)^2 = 0,$$

where $A = 3\alpha_2/(256a^2)$, $B = (c^2 - \alpha_1)/16a$, $C = \alpha_3/4a$ and $\gamma(T) = e^{-T/T_0}$. Solving the quartic equation in φ_ξ, we get

$$\varphi_\xi^2 = \frac{-B\varphi^2\ln(\varphi) \pm \varphi^2\ln(\varphi)\sqrt{B^2 - 4A[-C\gamma(T)\varphi(\varphi - 2) + C_1]}}{2A}.$$

This is similarly written as

$$\begin{aligned}\frac{\varphi_\xi^2}{\varphi^2\ln(\varphi)} &= \frac{-B \pm \sqrt{4AC\gamma(T)\varphi(\varphi - 2) + B^2 - 4AC_1}}{2A} \\ &= \frac{-B \pm \sqrt{4AC\gamma(T)(\varphi - 1)^2 + B^2 - 4AC\gamma(T) - 4AC_1}}{2A}.\end{aligned} \tag{5.3}$$

Now, we are endowed with two cases to consider based on the term

$$\mathcal{D} := B^2 - 4AC\gamma(T) - 4AC_1, \tag{5.4}$$

where we consider the cases when $\mathcal{D}$ is zero or nonzero. It is well-known that, the latter case signifies one of the following: (i) equilibrium or steady state, (ii) invariant property, and/or (iii) energy conservation.

In the case when $\mathcal{D} = 0$,

$$\frac{B^2}{4AC} - C_1 = \gamma(T). \tag{5.5}$$

Eq (5.3) now reduces to

$$\frac{\varphi_\xi^2}{\varphi^2 \ln(\varphi)} = \frac{-B \pm 2\sqrt{AC\gamma(T)}(\varphi - 1)}{2A} \tag{5.6}$$

Upon further simplification and integration, one gets

$$\int_0^\xi \frac{1}{\varphi \ln \varphi \sqrt{\alpha + \beta(\varphi - 1)}} d\varphi(s) = \int_0^\xi ds = \xi, \tag{5.7}$$

where $\alpha = -B/(2A)$ and $\beta = \beta(T) = \sqrt{C\gamma(T)/A}$. As the integral form appeared to be difficult to evaluate, there is need for a numerical integration approach. The numerical implementation for the evaluation of the integral is left for future studies. However, instead we apply traditional numerical technique that solves both the equations for symmetric and nonsymmetric potentials (2.7) and (5.1).

5.1. Numerical scheme implementation

Here, we present the numerical scheme used to approximate the solutions of the continuum DNA models with symmetric and nonsymmetric potentials; these are (2.7) and (5.1). The governing equations are obviously nonlinear hyperbolic partial differential equations, and we employ a finite difference method for spatial discretization and an explicit time-stepping scheme for temporal evolution. These are presented in the following subsections.

5.1.1. Spatial and temporal discretization

Let the computational domain be discretized as: On an interval $[-L/2, L/2]$ of length L, take

$$z_i = -\frac{L}{2} + i\Delta z, \quad i = 1, 2, \ldots, N_x,$$

$$t^n = n\Delta t, \quad n = 0, 1, 2, \ldots, N_t.$$

We denote the numerical approximation of $y(z, t)$ by:

$$y_i^n \approx y(z_i, t^n).$$

Finite difference approximations. The first-order spatial derivative:

$$\left(\frac{\partial y}{\partial z}\right)_i^n \approx \frac{y_{i+1}^n - y_{i-1}^n}{2\Delta z}.$$

Second-order spatial derivative is approximated by

$$\left(\frac{\partial^2 y}{\partial z^2}\right)_i^n \approx \frac{y_{i+1}^n - 2y_i^n + y_{i-1}^n}{(\Delta z)^2}.$$

Second-order time derivative approximated by

$$\left(\frac{\partial^2 y}{\partial t^2}\right)_i^n \approx \frac{y_i^{n+1} - 2y_i^n + y_i^{n-1}}{(\Delta t)^2}.$$

5.1.2. Discrete evolution scheme

Rewriting the governing equations yields the following symmetric model. Eq (2.7) is approximated numerically by

$$y_i^{n+1} = 2y_i^n - y_i^{n-1} + (\Delta t)^2 \left[C_i^n \, \delta_{zz} y_i^n + V_i^n\right], \tag{5.8}$$

where

$$C_i^n = \alpha_1 + 3\alpha_2 \left(\frac{y_{i+1}^n - y_{i-1}^n}{2\Delta z}\right)^2, \qquad V_i^n = 2a\gamma(T) e^{-2a(y_i^n)^2} \left(e^{-2a(y_i^n)^2} - 1\right) y_i^n.$$

Nonsymmetric model. Eq (5.1) is readily approximated by

$$y_i^{n+1} = 2y_i^n - y_i^{n-1} + (\Delta t)^2 \left[C_i^n \, \delta_{zz} y_i^n + \widetilde{V}_i^n\right], \tag{5.9}$$

where

$$\widetilde{V}_i^n = 2a\gamma(T) e^{-2ay_i^n} \left(e^{-2ay_i^n} - 1\right).$$

For the initial-boundary conditions, we consider Schwartz-type initial data:

$$y(z,0) = e^{-z^2}, \quad \frac{\partial y}{\partial t}(z,0) = 0.$$

Periodic boundary conditions are implemented:

$$y_0^n = y_{N_x}^n, \quad y_{N_x+1}^n = y_1^n.$$

The energy and mass functionals are respectively approximated as

$$E(t^n) = \sum_{i=1}^{N_x} \left[\frac{1}{2}(v_i^n)^2 + \frac{\alpha_1}{2}\left(\frac{\partial y}{\partial z}\right)_i^2 + \frac{\alpha_2}{2}\left(\frac{\partial y}{\partial z}\right)_i^4 + V(y_i^n)\right] \Delta z, \tag{5.10}$$

$$M(t^n) = \sum_{i=1}^{N_x} (y_i^n)^2 \Delta z. \tag{5.11}$$

where $V(y) = \gamma(T)\left(1 - e^{-2ay^2}\right)^2$.

To assess numerical accuracy, we compute

$$\text{Error}(t^n) = \frac{\|y^n - y^{\text{ref}}\|_2}{\|y^{\text{ref}}\|_2}, \tag{5.12}$$

where y^{ref} is the reference (initial Gaussian) solution.

A perturbed solution $\tilde{y}$ is introduced:

$$\tilde{y}(z,0) = y(z,0) + \varepsilon\xi(z),$$

where $\varepsilon \ll 1$.

The stability indicator is defined as

$$S(t^n) = \|y^n - \tilde{y}^n\|_2. \tag{5.13}$$

Growth of $S(t^n)$ indicates instability, while bounded behaviour suggests stable breather dynamics.

5.2. Numerical simulations

Numerical simulations of the solution to the Eq (5.1) with its mass and energy evolutions using the initial data $u(0, z) = A \exp(-z^2)\,\mathrm{sech}^{\,2}(z)$ are shown in Figure 9.

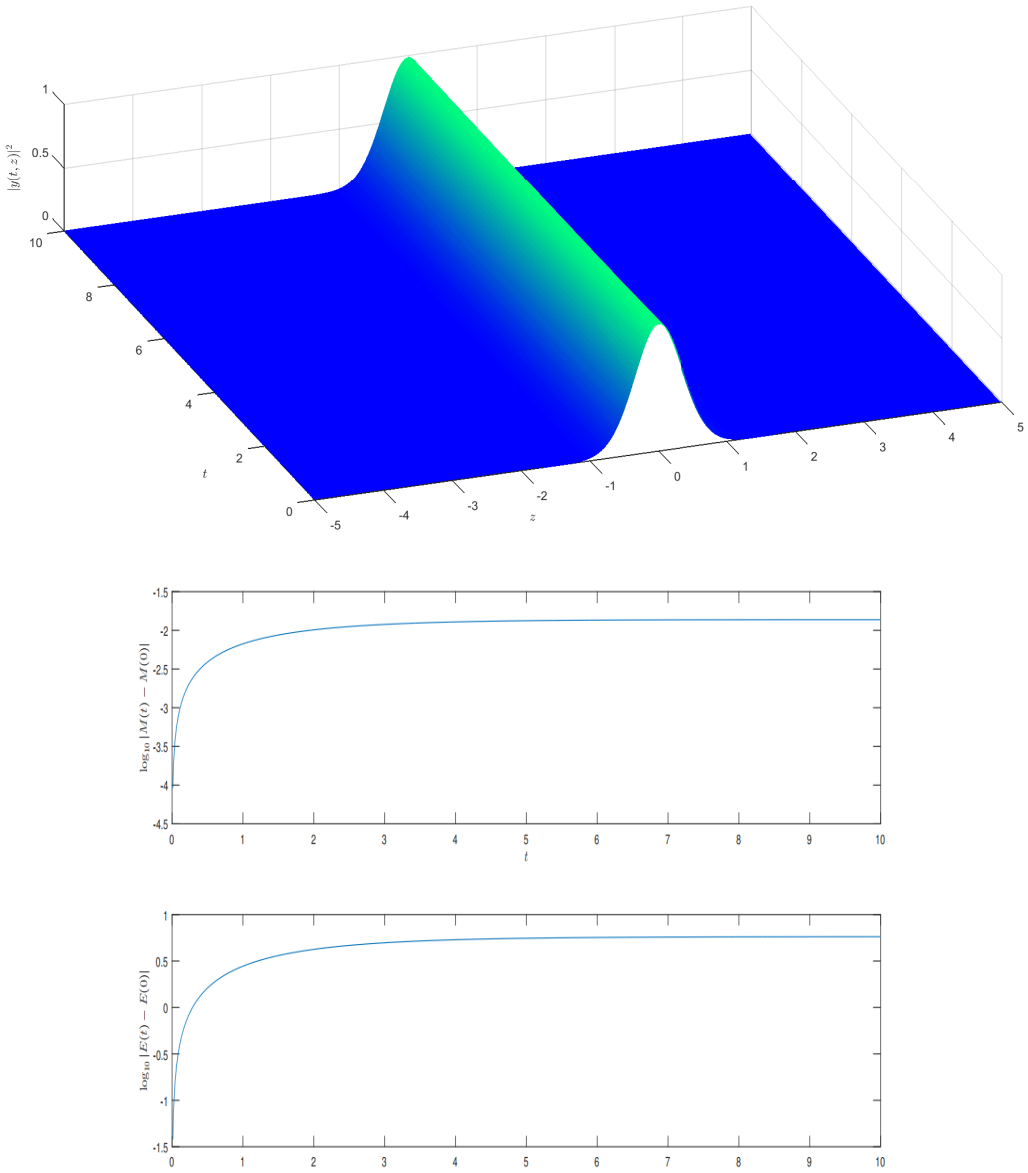

Figure 9. Top: Evolution of $|y(t, z)|^2$ of the evolution Eq (5.1) with initial data $e^{-z^2}\,\mathrm{sech}^{\,2}(z)$. Bottom: The evolution of mass and energy conservation.

Numerical solutions of the two Eqs (2.7) and (5.1) with different initial data, specifically Gaussian e^{-z^2} via the finite difference scheme, suggest travelling wave soltutions exhibiting symmetric and nonsymmetric properties. These properties are reflected as shown in Figure 10.

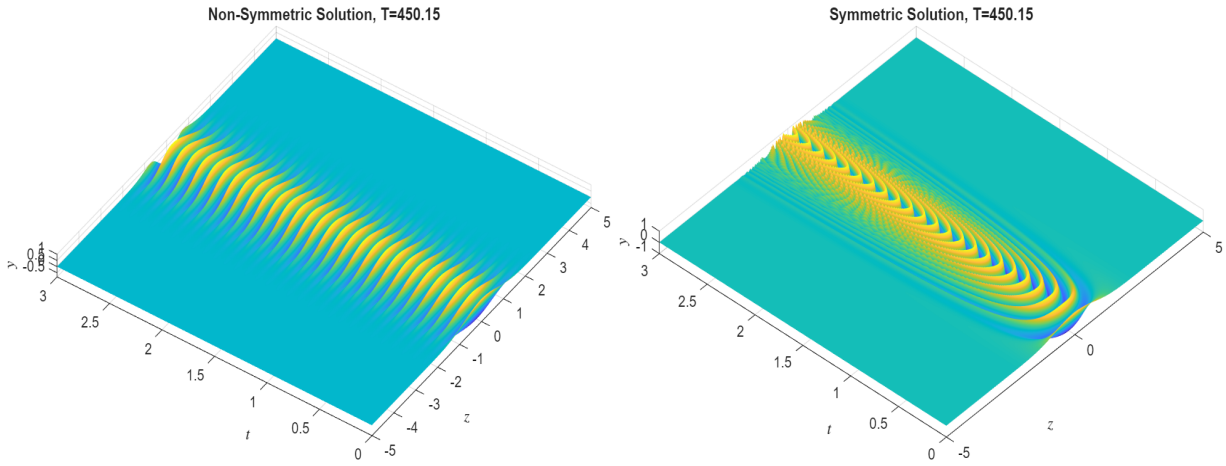

Figure 10. Numerical solutions $y(t, z)$ for symmetric and nonsymmetric Morse potentials with initial data e^{-z^2} via RK4 scheme.

5.3. Numerical validation

To support the analytical findings, we numerically simulate the governing equation using a finite difference scheme. The results confirm the persistence of localized breather-like structures and demonstrate their stability over time. The numerical profiles exhibit periodic energy exchange, consistent with the theoretical predictions.

The Figures 11, for symmetric (left) and nonsymmetric (right), show solutions at the final time $t = 12$ unit, for different temperatures 293.15–450.15 in Kelvin. A significant retardation in the DNA profile is observed for the nonsymmetric potential with increase in T, Figure 11 (right).

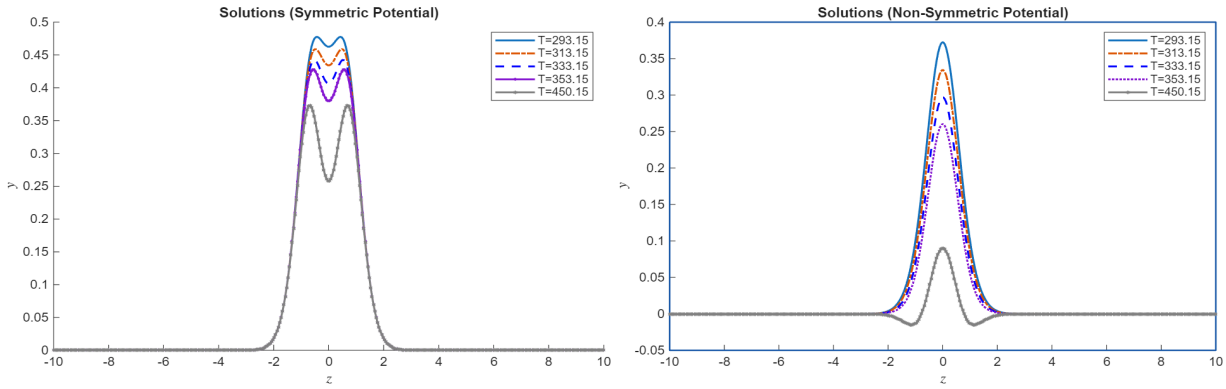

Figure 11. Solutions $y(t, z)$ for symmetric (left) and nonsymmetric (right) potentials at $t = 12$ for several T's values.

The evolutions of mass and energy at different values of T are shown in Figure 12.

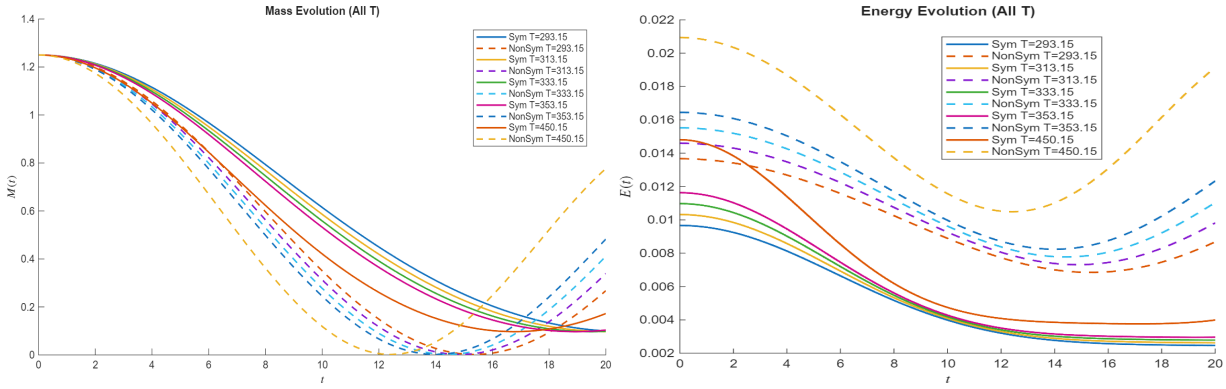

Figure 12. Evolutions of mass and energy $y(t, z)$ for symmetric (left) and nonsymmetric (right) potentials at different temperature values T and $D_e(T) = 1 + T/2$.

The 3D plots of the solutions for both symmetric and non-symmetric potentials are shown in Figures 10 and 13.

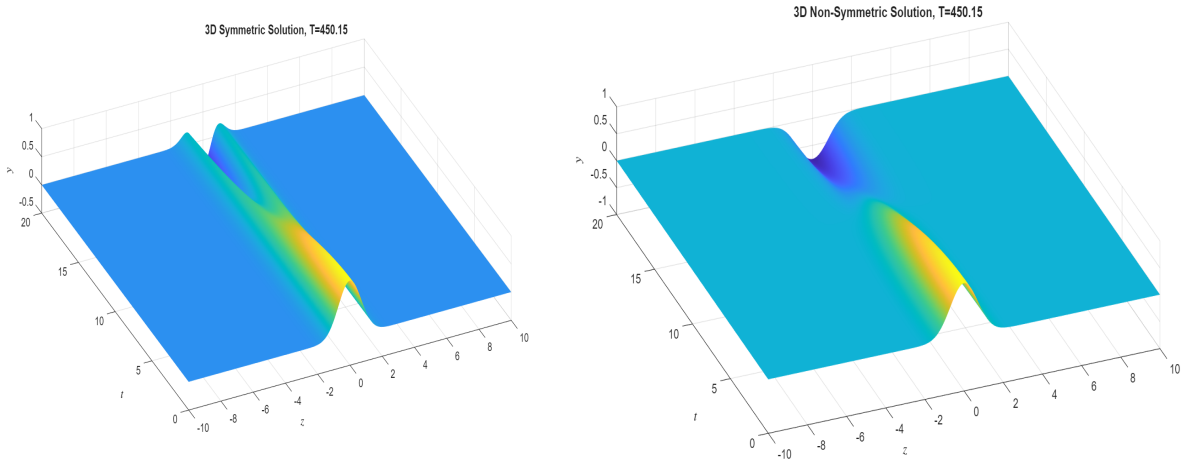

Figure 13. Solutions of $y(t, z)$ for symmetric (left) and nonsymmetric (right) potentials at the temperature value $T = 450.15$K with $D_e(T) = 1 + T/2$.

5.4. Stability analysis of breather solutions

To assess the stability of the obtained breather solutions, we introduce a small perturbation to the initial condition and examine its evolution over time. Let

$$y(z, 0) \to y(z, 0) + \varepsilon\eta(z),$$

where $\varepsilon \ll 1$.

A Lyapunov-type stability indicator is defined as

$$\Delta(t) = \|y(z, t) - y_{\text{pert}}(z, t)\|.$$

Numerical results, in Figure 14, show that for moderate parameter values, $\Delta(t)$ remains bounded, indicating that the breather solutions are dynamically stable. However, for higher temperature values, $\Delta(t)$ exhibits exponential growth, suggesting instability induced by thermal effects.

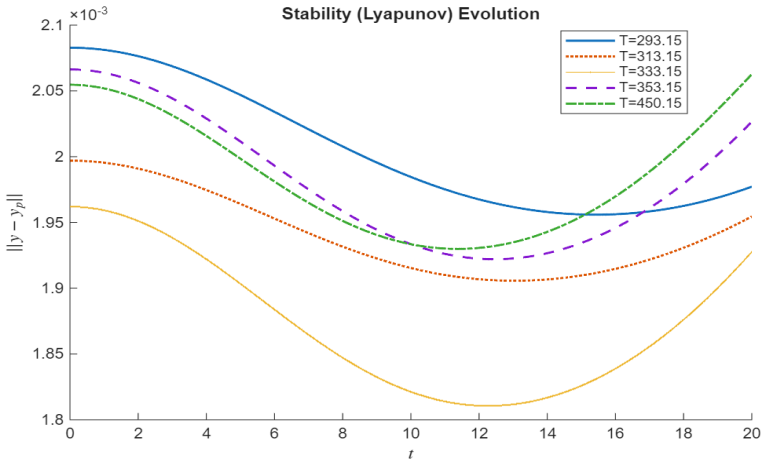

Figure 14. Stability of the solution $y(t, z)$ for symmetric potential at different temperature values T.

6. Discussion and conclusions

The derived mathematical model provides information on the process of predicting DNA dynamics. The vibrational dynamics of DNA given by Eq (2.7) are shown to be influenced by temperature. The variation of the function $D_e(T)$, the dissociation energy, is responsible for the stable behaviour of the dynamics. It is evident from the definitions of $D_e(T)$ and $\alpha(T)$ that they influence the solitary wave of the underlying dynamical equation. This observation is consistent with the temperature-induced denaturation of DNA seen in experiments. The presence of radiative wave in the dynamics has been established, which is in-line with the propagation of waves under the influence of external force; see Figures 5 and 7. Our study shows that it is possible to predict DNA behaviour under different heat settings using the derived model, which paves the way to understanding the theoretical framework for DNA's dynamics. The symmetric and nonsymmetric settings differ only in the process of replication, a remarkable behaviour in DNA. See Figure 13.

Numerical simulations reveal that increasing temperature enhances nonlinear interactions and modifies the stability of breather solutions. In particular, higher temperature values lead to increased oscillatory behaviour and may induce instability in the system.This is shown in 14.

In conclusion, solitary wave packets and radiative wave packets, with temperature dependence, are found by superpositioning of nonlinear solitons. A 1-soliton is observed to travel, and all of the sudden, a smaller wave packet emerges (like a ghost) and continues to grow while the existing wave packet diminishes. In addition, radiative behaviour is being observed in the DNA. This and other findings provide important novel information for the study of DNA dynamics by highlighting the significant effect of temperature. A modification of the proposed model that takes into account several environmental factors would provide a better understanding of the dynamical behaviour of DNA and improve both theoretical and experimental results.

Author contributions

All authors contributed to the investigation of DNA dynamics using variational principles and continuum approximation methods. The team collaboratively developed the theoretical framework, derived wave-packet and breather-soliton solutions, analyzed temperature effects, and interpreted the physical implications of the results. Here's the breakdown of the individual contributions: Umar M. Dauda: Conceptualization of the study, development of the mathematical model, analytical derivations, numerical simulations, data interpretation, manuscript writing, and correspondence with the journal. Hanita Daud: Supervision, validation of methodology, critical review of analytical results, and contribution to manuscript revision, source of funding. Hadil Alhazmi: Assistance in model formulation, computational analysis, validation of numerical results, and review of the manuscript. Nazreen Waeleh: Contribution to numerical implementation, data analysis, visualization of results, and technical editing of the manuscript. Sani Saleh Musa: Literature review, assistance in theoretical analysis, formatting, proofreading, and final manuscript preparation.

Use of Generative-AI tools declaration

The authors declare they have used Artificial Intelligence (AI) tools in the creation of this article. Microsoft Copilot is utilised to source relevant articles for an up-to-date knowledge of the literature and to avoid reproduction of same findings. The literature review sections were generated with the help of the said AI tool from the list of suggested articles; these are confirmed before listed in the reference section. Grammatical errors were corrected too. The MATLAB codes as used were debugged with the help of the tool.

Acknowledgments

The authors would like to express their sincere appreciation to Universiti Teknologi PETRONAS (UTP) for its continuous support through the SMARTDrive@UTP–Sustainable Mobility Advanced Research & Technology Program in collaboration with Diamond Gas Holding, a subsidiary of Mitsubishi Corporation (Malaysia branch). The authors also extend their gratitude to Universiti Teknikal Malaysia Melaka (UTeM) for its support and collaboration. In addition, the authors would like to thank Princess Nourah bint Abdulrahman University Researchers Supporting Project with project number (PNURSP2026R528), Princess Nourah bint Abdulrahman University, Riyadh, Saudi Arabia.

Conflict of interest

The authors declare that no conflicts of interest in this paper.

References

1. M. A. Aguero, M. De Lourdes Najera, M. Carrillo, Nonclassical solitonic structures in DNA's vibrational dynamics, *Int. J. Mod. Phys. B*, **22** (16), 2571–2582. https://doi.org/10.1142/S021797920803968X

2. R. Abazari, S. Jamshidzadeh, G. Wang, Mathematical modeling of DNA vibrational dynamics and its solitary wave solutions, *Rev. Mex. Fís.*, **64** (2018), 590–597. https://doi.org/10.31349/revmexfis.64.590 .
3. A. Chabchoub, A. Slunyaev, N. Hoffmann, F. Dias, B. Kibler, G. Genty, et al., The peregrine breather on the ZeroBackground limit as the two-soliton degenerate solution: An experimental study, *Front. Phys.*, **9** (2021), 633549. https://doi.org/10.3389/fphy.2021.633549
4. U. M. Dauda, M. A. Lawan, I. A. Auwal, M. M. Yusuf, On coupled time-fractional hea-equations, *Bayero J. Pure Appl. Sci.*, **16** (2023), 53.
5. S. W. Englander, N. R. Kallenbach, A. J. Heeger, J. A. Krumhansl, S. Litwin, Nature of the open state in long polynucleotide double helices: Possibility of soliton excitations, *Proc. Nat. Acad. Sci. USA*, **77** (1980), 7222–7226. https://doi.org/10.1073/pnas.77.12.7222
6. E. Clementi, S. Chin, *Structure and dynamics of nucleic acids, proteins, and Membranes*, New York: Springer, 1986. https://doi.org/10.1007/978-1-4684-5308-9
7. S. M. Lindsay, Low frequency coherent vibrations of DNA: The role of the hydration shell and phosphate-phosphate interactions, In: *Structure and dynamics of nucleic acids, proteins, and membranes*, New York: Springer, 1986. https://doi.org/10.1007/978-1-4684-5308-9_18
8. K. C. Lu, E. W. Prohofsky, L. L. Van Zandt, Vibrational modes of A-DNA, B-DNA, and A-RNA backbones: An application of a green-function refinement procedure, *Biopolymers*, **16** (1977), 2491–506. https://doi.org/10.1002/bip.1977.360161112
9. J. Lenhard, S. Hasse, H. Hasse, On the history of the Lennard-Jones potential, *Ann. Phys.*, **536** (2024), 2400115. https://doi.org/10.1002/andp.202400115
10. J. E. Lennard-Jones, Cohesion, *Proc. Phys. Soc.*, **43** (1931), 461. https://doi.org/10.1088/0959-5309/43/5/301
11. M. Mohammad, R. Nematollah, A. Azizollah, Radiative properties of Kinks in the $sin^4(\varphi)$ system, *Prog. Theor. Phys.*, **128** (2012), 615–627. https://doi.org/10.1143/PTP.128.615
12. P. M. Morse, Diatomic molecules according to the wave mechanics, II. Vibrational levels, *Phys. Rev.*, **34** (1929), 57. https://doi.org/10.1103/PhysRev.34.57 .
13. M. Peyrard, A. R. Bishop, Statistical mechanics of a nonlinear model for DNA denaturation, *Phys. Rev. Lett.*, **62** (1989), 2755–2758. https://doi.org/10.1103/PhysRevLett.62.2755
14. A. J. Stone, *The theory of intermolecular forces*, Oxford University Press, 1996.
15. S. S. Sabo, U. M. Dauda, S. Babuba, A. B. Bakari, On nonlinear biharmonic dispersive wave equations, *Fudma J. Sci.*, **9** (2025), 87–100.
16. S. Takeno, S. Homma, Topological solitons and modulated structure of bases in DNA double helices, *Prog. Theor. Phys.*, **70** (1983), 308–311.
17. U. M. Dauda, S. S. Musa. F. K. Iyanda, Dynamics of DNA: Nonlinear interaction of solitions, Available at SSRN: 4929897, 2024.
18. J. D. Watson, F. H. C. Crick, A structure for deoxyribose nucleic acid, *Nature*, **71** (1953), 733–738.

19. R. M. Wartell, A. S. Benight, Thermal denaturation of DNA molecules: A copmarison of theory with experiment, *Phys. Rep.*, **126** (1985), 67–107. https://doi.org/10.1016/0370-1573(85)90060-2

20. L. V. Yakushevich, The effect of damping, external fields and inhomogeneity on the nonlinear dynamics of biopolymers, *Stud. Biophys.*, **121** (1987), 201–207.

21. L. V. Yakushevich, Nonlinear DNA dynamics: A new model, *Phys. Lett. A*, **136** (1989), 413–417. https://doi.org/10.1016/0375-9601(89)90425-8

22. L. V. Yakushevich, *Nonlinear hysics of DNA, 2nd Edition*, 2006.

23. L. V. Yakushevich, *Nonlinear physics of DNA*, John Wiley & Sons, 2004.

24. L. Najera, M. Carrillo, M. A. Agöuero, Non-classical solitons and the broken hydrogen bonds in DNA vibrational dynamics, *Adv. Studies Theor. Phys.*, **4** (2010), 495–510.

25. V. G. Ivancevic, T. T. Ivancevic, Sine-Gordon solitons, kinks and breathers as physical models of nonlinear excitations in living cellular structures. https://arxiv.org/pdf/1305.0613

Supplementary: MATLAB CODE

```
%% CONTINUUM DNA MODELS (SYMMETRIC & NON-SYMMETRIC)

clear; clc;

% Interpreter
Intp = 'Interpreter';  Ltx= 'Latex';

% Domain
L = 20; Nx = 400;
dz = L/Nx;
z = linspace(-L/2, L/2, Nx);

% Time
dt = 0.0015; Nt = 2000;
tmax = dt*Nt;
tvec = (1:Nt)*dt;

% Parameters
k1 = 0.23;  k2 = 0.0623;
h = 0.01;   m = 230*1;

alpha1 = k1*h^2/m;
alpha2 = k2*h^4/m;
a = 0.1;

```

```
% Temperature sweep
Tvals = [293.15, 313.15, 333.15, 353.15, 450.15];

% FIGURES
figure(1); hold on; title('Solutions (Symmetric Potential)');
figure(2); hold on; title('Solutions (Non-Symmetric Potential)');
figure(3); hold on; title('Energy Evolution (All T)');
figure(4); hold on; title('Mass Evolution (All T)');
figure(5); hold on; title('Relative Error Evolution');
figure(6); hold on; title('Stability Evolution');

for T = Tvals

De = 1 + 0.5*T.^3; %1 + 0.5*T; %-1 + T.^2 + 0.5*T.^3;
gamma = De/(2*m);

% Initial condition
y = exp(-z.^2); v = zeros(size(z));
y_ns = y; v_ns = v;   % non-symmetric

% Exact (reference) solution
y_exact = exp(-z.^2);

Energy = zeros(1,Nt); Mass = zeros(1,Nt);
Energy_ns = zeros(1,Nt); Mass_ns = zeros(1,Nt);
Error = zeros(1,Nt);
Stability = zeros(1,Nt);

% Storage for 3D plots
Ysurf = zeros(Nt, Nx);
Ysurf_ns = zeros(Nt, Nx);

% Perturbed (for stability)
y_pert = y + 1e-4*randn(size(z)); v_pert = v;

for n = 1:Nt

%% SYMMETRIC POTENTIAL MODEL
yz = (circshift(y,-1)-circshift(y,1))/(2*dz);
yzz = (circshift(y,-1)-2*y+circshift(y,1))/(dz^2);

```

```
        coeff = alpha1 + 3*alpha2*(yz.^2);
        V = 2*a*gamma .* exp(-2*a*y.^2) .* (exp(-2*a*y.^2)-1).*y;

        ytt = coeff .* yzz + V;

        v = v + dt*ytt;
        y = y + dt*v;

        %% NON-SYMMETRIC POTENTIAL MODEL
        yz_ns = (circshift(y_ns,-1)-circshift(y_ns,1))/(2*dz);
        yzz_ns = (circshift(y_ns,-1)-2*y_ns+circshift(y_ns,1))/(dz
           ^2);

        coeff_ns = alpha1 + 3*alpha2*(yz_ns.^2);
        V_ns = 2*a*gamma .* exp(-2*a*y_ns) .* (exp(-2*a*y_ns)-1);

        ytt_ns = coeff_ns .* yzz_ns + V_ns;

        v_ns = v_ns + dt*ytt_ns;
        y_ns = y_ns + dt*v_ns;

        %% Stability
        yz_p = (circshift(y_pert,-1)-circshift(y_pert,1))/(2*dz);
        yzz_p = (circshift(y_pert,-1)-2*y_pert+circshift(y_pert,1))
           /(dz^2);

        coeff_p = alpha1 + 3*alpha2*(yz_p.^2);
        V_p = 2*a*gamma .* exp(-2*a*y_pert.^2) .* (exp(-2*a*y_pert
           .^2)-1).*y_pert;

        ytt_p = coeff_p .* yzz_p + V_p;

        v_pert = v_pert + dt*ytt_p;
        y_pert = y_pert + dt*v_pert;

        Stability(n) = norm(y - y_pert);

        %% Energy & Mass
        yz = (circshift(y,-1)-circshift(y,1))/(2*dz);
        Energy(n) = sum(0.5*v.^2 + 0.5*alpha1*yz.^2 + ...
        0.5*alpha2*yz.^4 + gamma*(1-exp(-2*a*y.^2)).^2)*dz;
        Mass(n) = sum(y.^2)*dz;
```

```
        yz_ns = (circshift(y_ns,-1)-circshift(y_ns,1))/(2*dz);
        Energy_ns(n) = sum(0.5*v_ns.^2 + 0.5*alpha1*yz_ns.^2 + ...
        0.5*alpha2*yz_ns.^4 + gamma*(1-exp(-2*a*y_ns)).^2)*dz;
        Mass_ns(n) = sum(y_ns.^2)*dz;

        % Relative Error
        Error(n) = norm(y - y_exact)/norm(y_exact);

        % Store surfaces
        Ysurf(n,:) = y;
        Ysurf_ns(n,:) = y_ns;
        end

        % PLOTS (ALL IN ONE WITH LEGEND)
        figure(1); plot(z,y,'DisplayName',['T=',num2str(T)]);
        figure(2); plot(z,y_ns,'DisplayName',['T=',num2str(T)]);

        figure(3); plot(tvec,Energy,'DisplayName',['Sym T=',num2str
           (T)]);
        plot(tvec,Energy_ns,'--','DisplayName',['NonSym T=',num2str
           (T)]);

        figure(4); plot(tvec,Mass,'DisplayName',['Sym T=',num2str(T
           )]);
        plot(tvec,Mass_ns,'--','DisplayName',['NonSym T=',num2str(T
           )]);

        figure(5); plot(tvec,Error,'DisplayName',['T=',num2str(T)])
           ;

        figure(6); semilogy(tvec,Stability,'DisplayName',['T=',
           num2str(T)]);

        % 3D SURFACE PLOTS
        figure;
        surf(z,tvec,Ysurf); shading interp;
        title(['3D Symmetric Solution, T=',num2str(T)]);
        xlabel('$z$',Intp,Ltx); ylabel('$t$',Intp,Ltx); zlabel('$y$
           ',Intp,Ltx);

        figure;
        surf(z,tvec,Ysurf_ns); shading interp;
        title(['3D Non-Symmetric Solution, T=',num2str(T)]);
```

```
143         xlabel('$z$',Intp,Ltx); ylabel('$t$',Intp,Ltx); zlabel('$y$
                ',Intp,Ltx);
144         end
145
146         % Add legends & labels
147         figure(1); legend; xlabel('$z$',Intp,Ltx); ylabel('$y$',
                Intp,Ltx);
148         % title('Solutions (Symmetric Potential)');
149
150         figure(2); legend; xlabel('$z$',Intp,Ltx); ylabel('$y$',
                Intp,Ltx);
151         % title('Solutions (Non-Symmetric Potential)');
152         figure(3); legend; xlabel('$t$',Intp,Ltx); ylabel('$E(t)$',
                Intp,Ltx);
153         % title('Energy Evolution (All T)');
154         figure(4); legend; xlabel('$t$',Intp,Ltx); ylabel('$M(t)$',
                Intp,Ltx);
155         % title('Mass Evolution (All T)');
156         figure(5); legend; xlabel('$t$',Intp,Ltx); ylabel('Error',
                Intp,Ltx);
157         % title('Relative Error Evolution');
158         figure(6); legend; xlabel('$t$',Intp,Ltx); ylabel('$||y-y_p
                ||$',Intp,Ltx);
159         % title('Stability Evolution');
```